NACA

RESEARCH MEMORANDUM

WIND-TUNNEL INVESTIGATION AT HIGH SUBSONIC SPEEDS OF THE STATIC LONGITUDINAL AND STATIC LATERAL STABILITY CHARACTERISTICS OF A WING-FUSELAGE COMBINATION HAVING A TRIANGULAR WING OF ASPECT RATIO 2.31 AND AN NACA 65A003 AIRFOIL

By James W. Wiggins

Langley Aeronautical Laboratory
Langley Field, Va.

NATIONAL ADVISORY COMMITTEE
FOR AERONAUTICS

WASHINGTON
August 28, 1953

NATIONAL ADVISORY COMMITTEE FOR AERONAUTICS

RESEARCH MEMORANDUM

WIND-TUNNEL INVESTIGATION AT HIGH SUBSONIC SPEEDS OF THE STATIC LONGITUDINAL AND STATIC LATERAL STABILITY CHARACTERISTICS OF A WING-FUSELAGE COMBINATION HAVING A TRIANGULAR WING OF ASPECT RATIO 2.31 AND AN NACA 65A003 AIRFOIL

By James W. Wiggins

SUMMARY

An investigation was conducted in the Langley high-speed 7- by 10-foot wind tunnel to determine the static longitudinal and static lateral stability characteristics of a wing-fuselage combination having a triangular wing of aspect ratio 2.31, and an NACA 65A003 airfoil section. The tests covered a Mach number range from 0.40 to 0.95 with the corresponding Reynolds numbers, based on the mean aerodynamic chord of the wing, ranging from 3×10^6 to 5×10^6. The results indicate that a pitch-up occurs at angles of attack of 11° or 12° (lift coefficient of approximately 0.60) for the clean-wing configuration within the Mach number range from 0.70 to 0.85. The addition of small notches in the leading edge of the wing at the 0.60-semispan station essentially eliminated the pitch-up at these angles of attack. A slight increase in drag coefficient was indicated for the notched-wing configuration at lift coefficients above 0.20 for Mach numbers of 0.70 and 0.91.

The directional instability of the model increased considerably at angles of attack above 18°. In general, Mach number effects at low lift coefficients on some of the more important stability derivatives and performance parameters were fairly small over the range investigated.

INTRODUCTION

The present investigation is a continuation of a program being conducted in the Langley high-speed 7- by 10-foot tunnel to determine the

[redacted]

[redacted]

effects of wing geometry on longitudinal and lateral stability characteristics of a wing-body configuration at Mach numbers up to 0.95. The characteristics in pitch and sideslip of a wing-fuselage combination having a triangular wing of aspect ratio 2.31 and an NACA 65A003 airfoil section are reported herein. Some pitch tests were made with a notch in the leading edge of the wing at the 0.60-semispan station. The data are presented with only a brief analysis in order to expedite publication. The characteristics in pitch and sideslip of the fuselage alone are presented in references 1 and 2, respectively.

SYMBOLS

The stability system of axes used for the presentation of the data, together with an indication of the positive directions of forces, moments, and angles, are presented in figure 1. All moments are referred to the projection of the quarter-chord point of the mean aerodynamic chord on the fuselage center line.

C_L	lift coefficient, Lift/qS
C_m	pitching-moment coefficient, Pitching moment/qS$\bar{c}$
C_D	drag coefficient, Drag/qS
C_l	rolling-moment coefficient, Rolling moment/qSb
C_n	yawing-moment coefficient, Yawing moment/qSb
L/D	lift-drag ratio, C_L/C_D
C_Y	lateral-force coefficient, Lateral force/qS
q_o	free-stream dynamic pressure, $\frac{\rho V^2}{2}$, lb/sq ft
ρ	mass density of air, slugs/cu ft
V	free-stream velocity, ft/sec
M	Mach number
R	Reynolds number
S_W	wing area, sq ft

S_B area of base of body, sq ft

b wing span, ft

$\bar{c}$ mean aerodynamic chord, ft

α angle of attack, deg

β angle of sideslip, deg

p_B pressure at base of body, lb/sq ft

p_o free-stream static pressure, lb/sq ft

$\Delta C_{D_{B.P.}}$ base-pressure drag coefficient, $\frac{p_B - p_o}{q_o}\frac{S_B}{S_W}$

$C_{l_\beta} = \frac{\partial C_l}{\partial \beta}$, per deg

$C_{n_\beta} = \frac{\partial C_n}{\partial \beta}$, per deg

$C_{Y_\beta} = \frac{\partial C_Y}{\partial \beta}$, per deg

$C_{L_\alpha} = \frac{\partial C_L}{\partial \alpha}$, per deg

$\frac{C_m}{C_L} = \frac{\partial C_m}{\partial C_L}$

MODEL AND APPARATUS

A drawing of the model investigated and details of the wing-leading-edge notches are shown in figure 2 along with a table of wing ordinates. The geometric characteristics of the body can be obtained from reference 1. The wing had a leading-edge sweep angle of 60°, aspect ratio of 2.31, and an NACA 65A003 airfoil section parallel to the free stream and was attached to the fuselage in a midwing position.

[redacted]

The model was tested on the sting support shown in figures 3 and 4. With this support the model can be remotely operated through an angle-of-attack range of 28°, in the plane of the vertical strut, at various established angles of sideslip (fig. 3). The model can be rolled 90° (fig. 4) at the coupling in the sting behind the model for tests at various established angles of attack through a sideslip-angle range from -14° to 14°. An internally mounted electrical strain-gage balance was used to measure all moments and forces.

TESTS AND CORRECTIONS

The tests were made in the Langley high-speed 7- by 10-foot tunnel through a Mach number range from 0.40 to 0.95. The blocking corrections which were applied were determined by the velocity-ratio method of reference 3.

The longitudinal characteristics were determined from tests in which the angle of attack was varied from -3° to 24°. Some of these tests were repeated with a notch (fig. 2) cut in the leading edge of the wing at the 0.60-semispan station. The sideslip tests were conducted at angles of attack of 0° and 6° and through an angle-of-sideslip range from -5° to 12°; also, tests were made throughout an angle-of-attack range from -3° to 24° at sideslip angles of ±4°.

The jet-boundary corrections, which were applied to the angle of attack and drag, were determined from reference 4.

Sting-support tares have been determined for tailless models generally similar to the present configuration and were found to be negligible for all forces and moments except drag. The drag tare results from the influence of the sting on the external pressures on the model particularly near the rearward end. The application of the tare drag would increase the total drag coefficient by about 0.002 throughout the test ranges of angle of attack and Mach number. The tare correction has not been applied to the data herein as some uncertainty exists regarding its exact magnitude and also because the correction was obtained after other related investigations (for example, refs. 1 and 5) had been published. All drag data have been corrected to the condition of a pressure at the fuselage base equal to the free-stream static pressure. This increment of base-pressure drag coefficient which was added to the drag data is presented in figure 5.

No corrections to account for aerolastic distortion have been applied to the data presented; however, these effects are believed to be small.

The angle of attack and the angle of sideslip have been corrected for the deflection of the sting-support system and balance under load.

The variation with Mach number of mean test Reynolds number (based on the mean aerodynamic chord of the wing) is presented in figure 6.

RESULTS AND DISCUSSION

The results of the investigation are presented in the following figures:

Data:	Figure
Basic, longitudinal	7 to 11
Lift-drag ratios	12
Basic, lateral	13 to 15
Lateral derivatives	16 to 18
Parameters at $\alpha = 0^\circ$	19

Longitudinal Stability Characteristics

The pitching-moment results presented in figures 8 and 9 for the clean-wing configuration indicate that a pitch-up occurs at an angle of attack of about 11° or 12° $\left(C_L \approx 0.60\right)$ at Mach numbers of 0.70, 0.80, and 0.85. Although this pitch-up is rather mild and short-lived when compared with swept wings of taper ratios other than 0 (ref. 5), it still is undesirable. In an attempt to eliminate or reduce this pitch-up, notches were cut in the leading edges of the wings at the 0.60-semispan station. The geometric characteristics of the notch were determined from a study of unpublished low-speed results on a 45° swept wing having an aspect ratio of 4 and a taper ratio of 0.6. The results presented in figures 8 and 9 show that the pitch-up was essentially eliminated by the notch at these angles of attack. However, the data indicate that a tendency to pitch up may still exist at an angle of attack of about 18° $\left(C_L \approx 0.90\right)$, although an unstable condition was not reached in these tests. Very little effect of the notch on the stability of the model is indicated at angles of attack and lift coefficients near zero.

The drag data of figure 11(b) show an increase in drag coefficient at lift coefficients above approximately 0.20 for the notched-wing configuration, particularly at Mach numbers of 0.70 and 0.91. This increase in drag at these lift coefficients is probably a result of the reduction in lift coefficient at comparable angles of attack for the notched-wing configuration (fig. 7). The preceding characteristics result in a slight reduction in the lift-drag ratios over the lift range discussed (fig. 12).

[redacted]

The drag data plotted against angle of attack (fig. 10) show a slight decrease in drag at the higher angles of attack for the notched-wing configuration.

Lateral Stability Characteristics

The variation of the lateral coefficients, C_n, C_Y, and C_l with angle of sideslip is shown in figures 13, 14, and 15, respectively. The slopes of C_{n_β}, C_{Y_β}, and C_{l_β} measured near an angle of sideslip of 0° are presented in figures 16, 17, and 18, respectively, and show good agreement with the values from the parameter tests.

The results presented in figure 16 indicate directional instability (negative values of C_{n_β}) at all angles of attack. A rapid increase in this instability occurs at angles of attack above 18° which is probably a result of wing-fuselage interference as indicated in reference 6. The instability shown at angles of attack up to 18° is primarily the unstable moment of the body shown by the body-alone results in reference 2.

The variation of the effective dihedral derivative C_{l_β} with angle of attack (fig. 18) is linear at the lower angles of attack; however, above an angle of attack of about 8°, the variation becomes somewhat erratic, particularly at the higher Mach numbers. This erratic variation is probably a result of asymmetrical stalling of the wing semispans while in an attitude of sideslip.

Mach Number Effects

The effects of Mach number on some of the more important stability derivatives and performance parameters at low lift coefficients are shown in figure 19. The aerodynamic center, indicated by $\frac{dC_m}{dC_L}$, moves rearward about 5 percent of the mean aerodynamic chord at the high subsonic Mach numbers. In general, Mach number effects were fairly small as might be expected for a thin low-aspect-ratio wing.

CONCLUSIONS

An investigation conducted in the Langley high-speed 7- by 10-foot wind tunnel to determine the static longitudinal and static lateral stability characteristics of a wing-fuselage configuration having a wing of

aspect ratio 2.31 and an NACA 65A003 airfoil section indicate the following specific conclusions:

1. Notches in the leading edge of the wing at the 0.60-semispan stations essentially eliminated the pitch-up of the model that occurred at angles of attack of 11° or 12° (lift coefficient of approximately 0.60).

2. A slight increase in drag coefficient was indicated for the notched-wing configuration at lift coefficients above 0.20 for Mach numbers of 0.70 and 0.91.

3. The directional instability (negative C_{n_β}) of the wing-fuselage configuration increased rapidly at angles of attack above 18°.

4. In general, Mach number effects at low lift coefficients on some of the more important stability derivatives and performance parameters were fairly small over the range investigated.

Langley Aeronautical Laboratory,
National Advisory Committee for Aeronautics,
Langley Field, Va., June 30, 1953.

[redacted]

REFERENCES

1. Kuhn, Richard E., and Wiggins, James W.: Wind-Tunnel Investigation of the Aerodynamic Characteristics in Pitch of Wing-Fuselage Combinations at High Subsonic Speeds. Aspect-Ratio Series. NACA RM L52A29, 1952.

2. Kuhn, Richard E., and Fournier, Paul G.: Wind-Tunnel Investigation of the Static Lateral Stability Characteristics of Wing-Fuselage Combinations at High Subsonic Speeds - Sweep Series. NACA RM L52G11a, 1952

3. Hensel, Rudolf W.: Rectangular-Wind-Tunnel Blocking Corrections Using the Velocity-Ratio Method. NACA TN 2372, 1951.

4. Gillis, Clarence L., Polhamus, Edward C., and Gray, Joseph L., Jr.: Charts for Determining Jet-Boundary Corrections for Complete Models in 7- by 10-Foot Closed Retangular Wind Tunnels. NACA WR L-123, 1945. (Formerly NACA ARR L5G31.)

5. King, Thomas J., Jr., and Pasteur, Thomas B.: Wind-Tunnel Investigation of the Aerodynamic Characteristics in Pitch of Wing-Fuselage Combinations at High Subsonic Speeds - Taper-Ratio Series. NACA RM L53E20, 1953.

6. Jacquet, Bryon M., and Brewer, Jack D.: Effects of Various Outboard and Central Fins on Low-Speed Static-Stability and Rolling Characteristics of a Triangular-Wing Model. NACA RM L9E18, 1949.

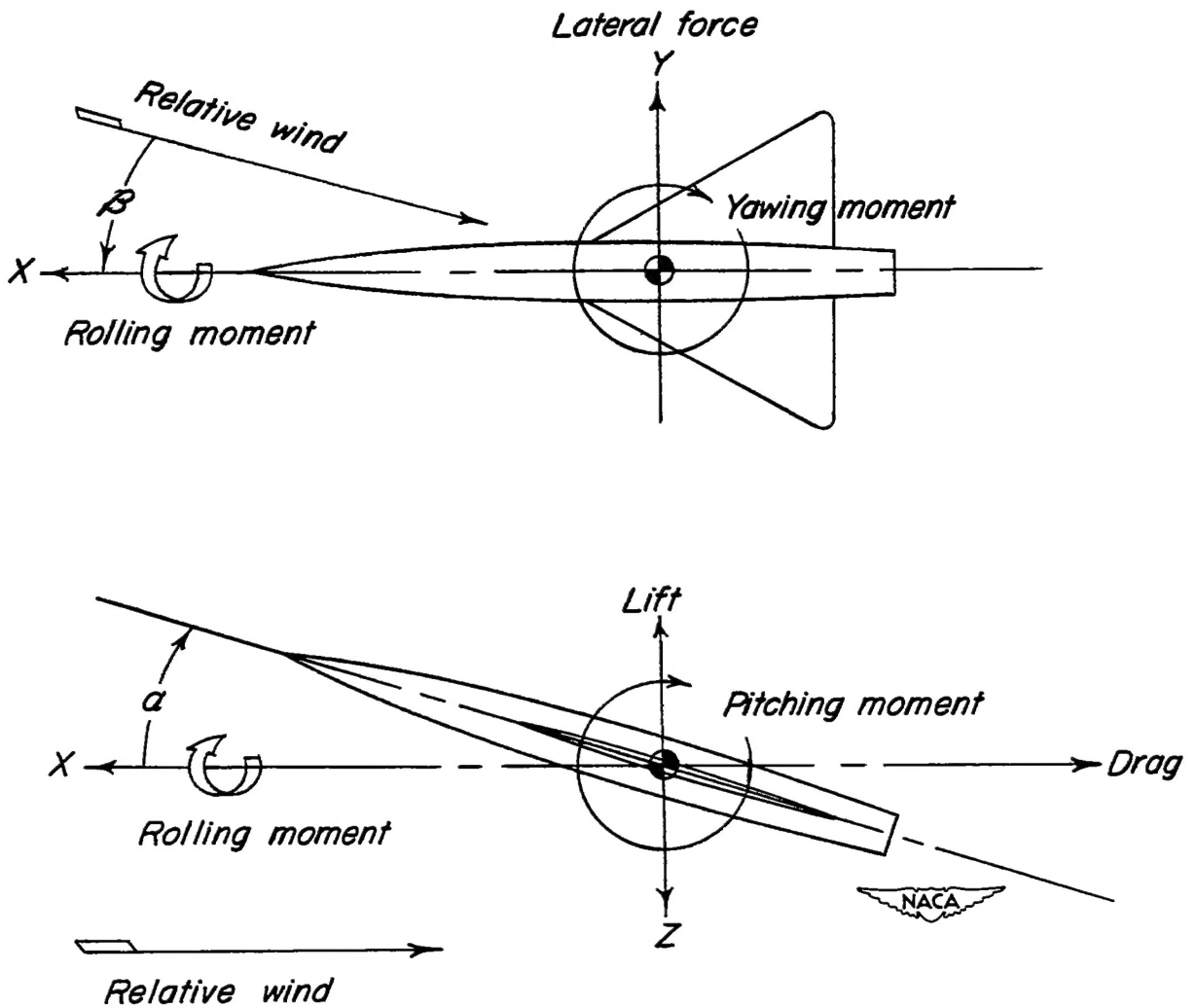

Figure 1.- System of axes used showing positive direction of forces, moments, and angles.

[redacted]

Wing ordinates	
X(%c)	Y(%c)
0	0
.50	.234
.75	.284
1.25	.362
2.50	.493
5.00	.658
7.50	.796
10.00	.912
15.00	1.097
20.00	1.236
25.00	1.342
30.00	1.420
35.00	1.472
40.00	1.498
45.00	1.497
50.00	1.465
55.00	1.402
60.00	1.309
65.00	1.191
70.00	1.053
75.00	.897
80.00	.727
85.00	.549
90.00	.369
95.00	.188
100.00	.007
L.E.R.	.057
T.E.R.	.0068

Wing Geometry

Area	2.25 sq ft
Aspect ratio	2.31
Sweep angle, $\bar{c}/4$	52.4°
Airfoil section parallel to plane of symmetry	NACA 65A003

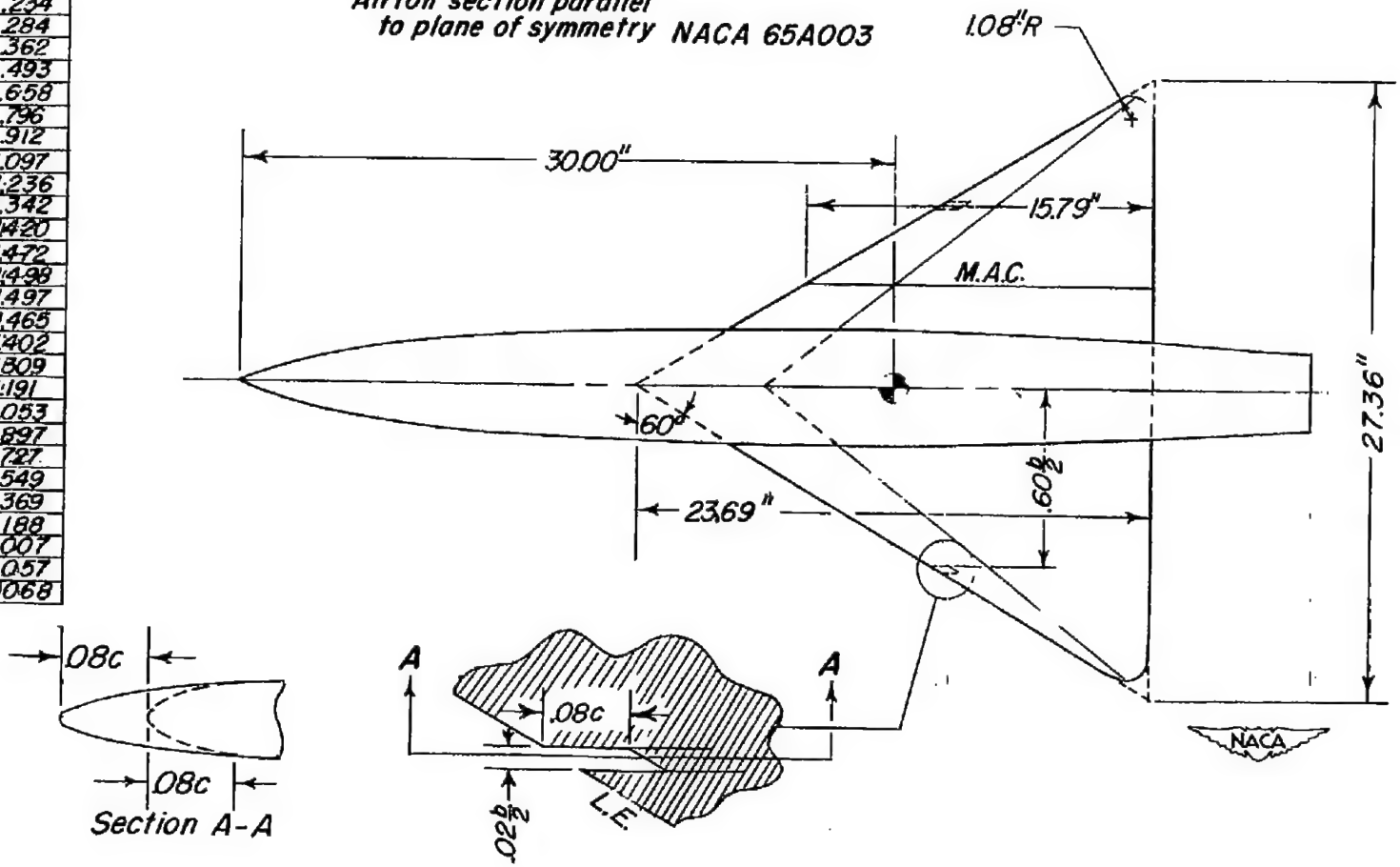

Figure 2.- Plan form of model showing details of notch in leading edge of wing.

L-79563

Figure 3.- Photograph of model on sting support mounted for angle-of-attack tests.

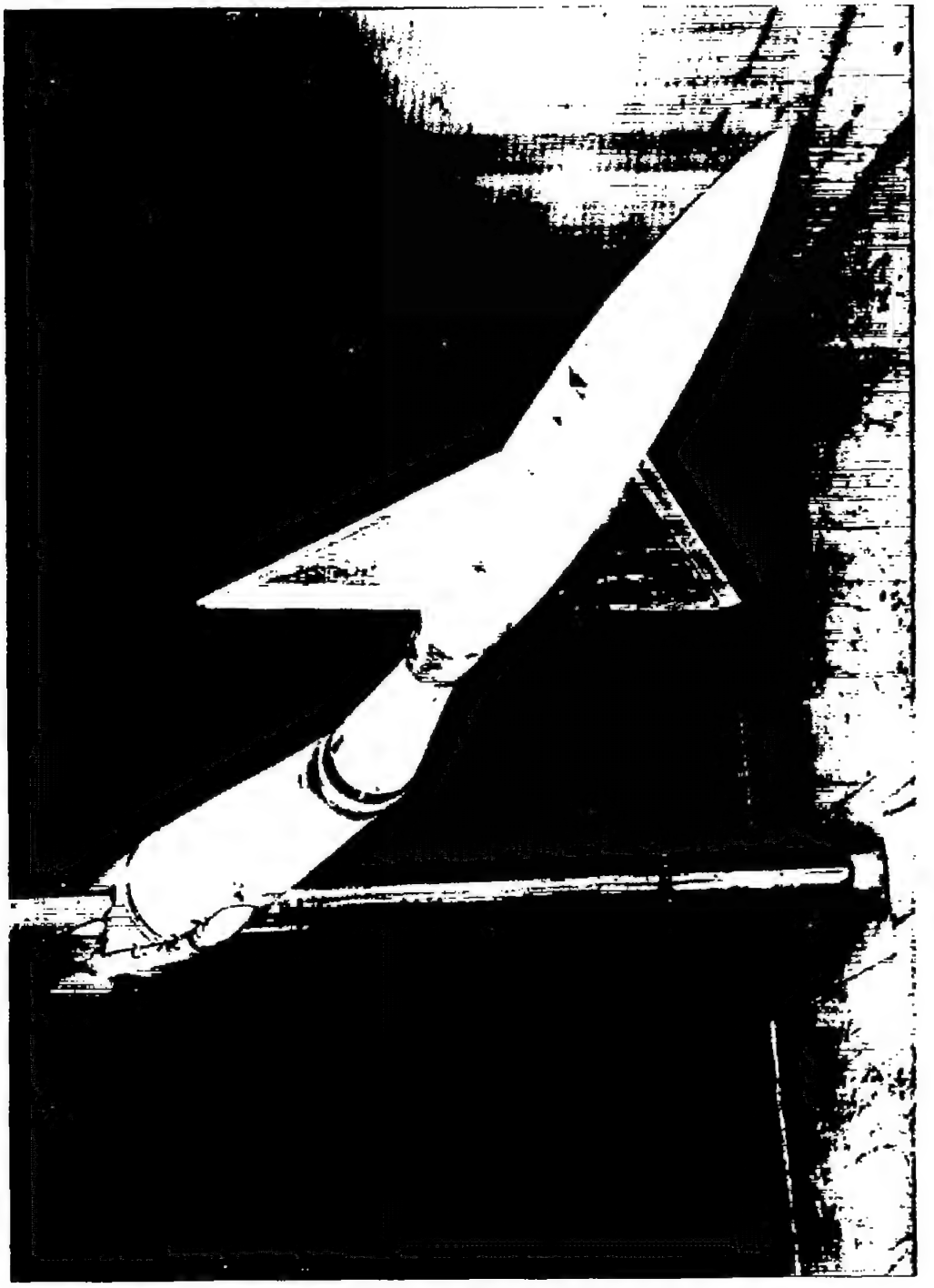

L-79564

Figure 4.- Photograph of model on sting support mounted for angle-of-sideslip tests.

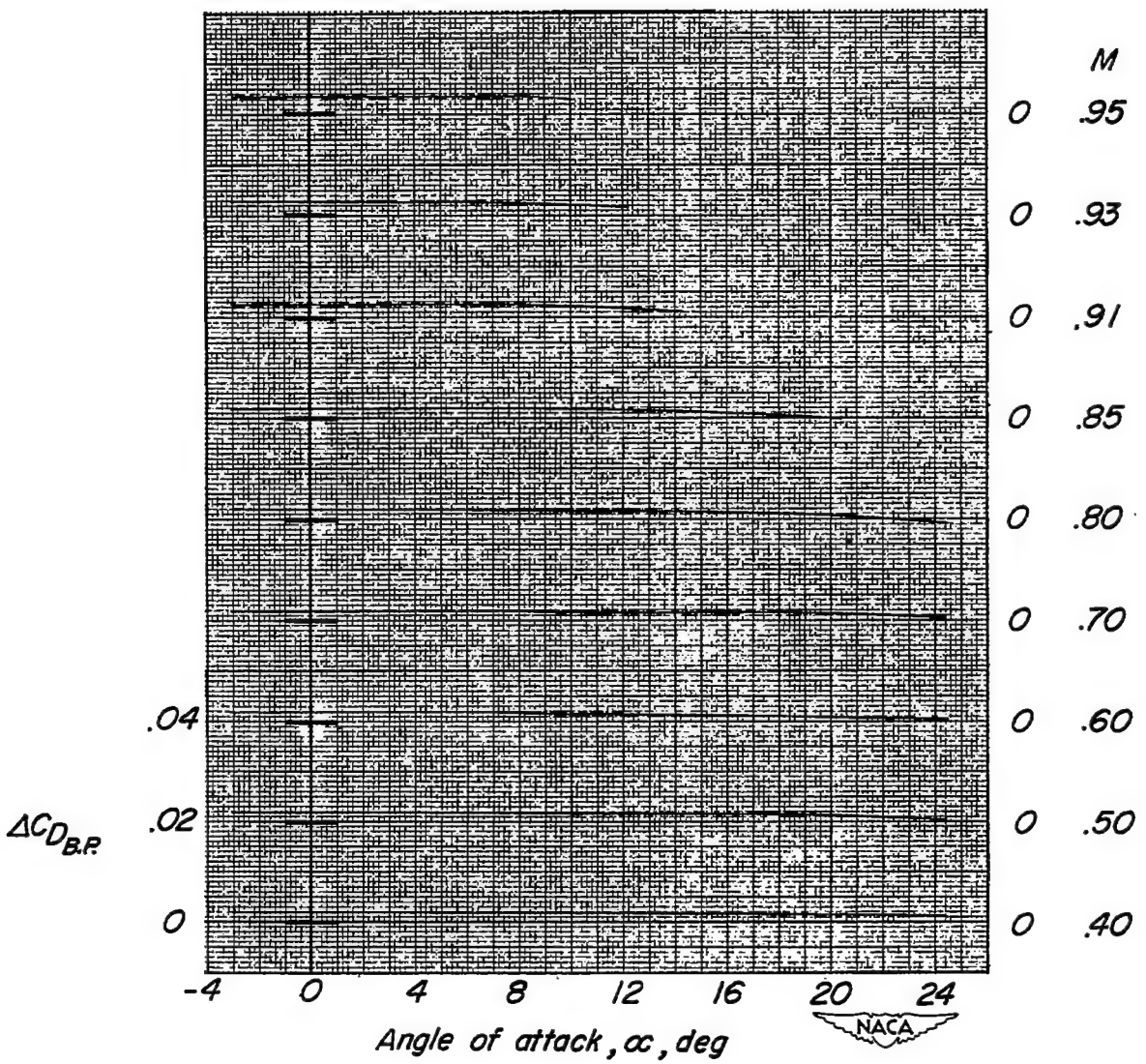

Figure 5.- Variation of base-pressure drag coefficient with angle of attack throughout the test Mach number range.

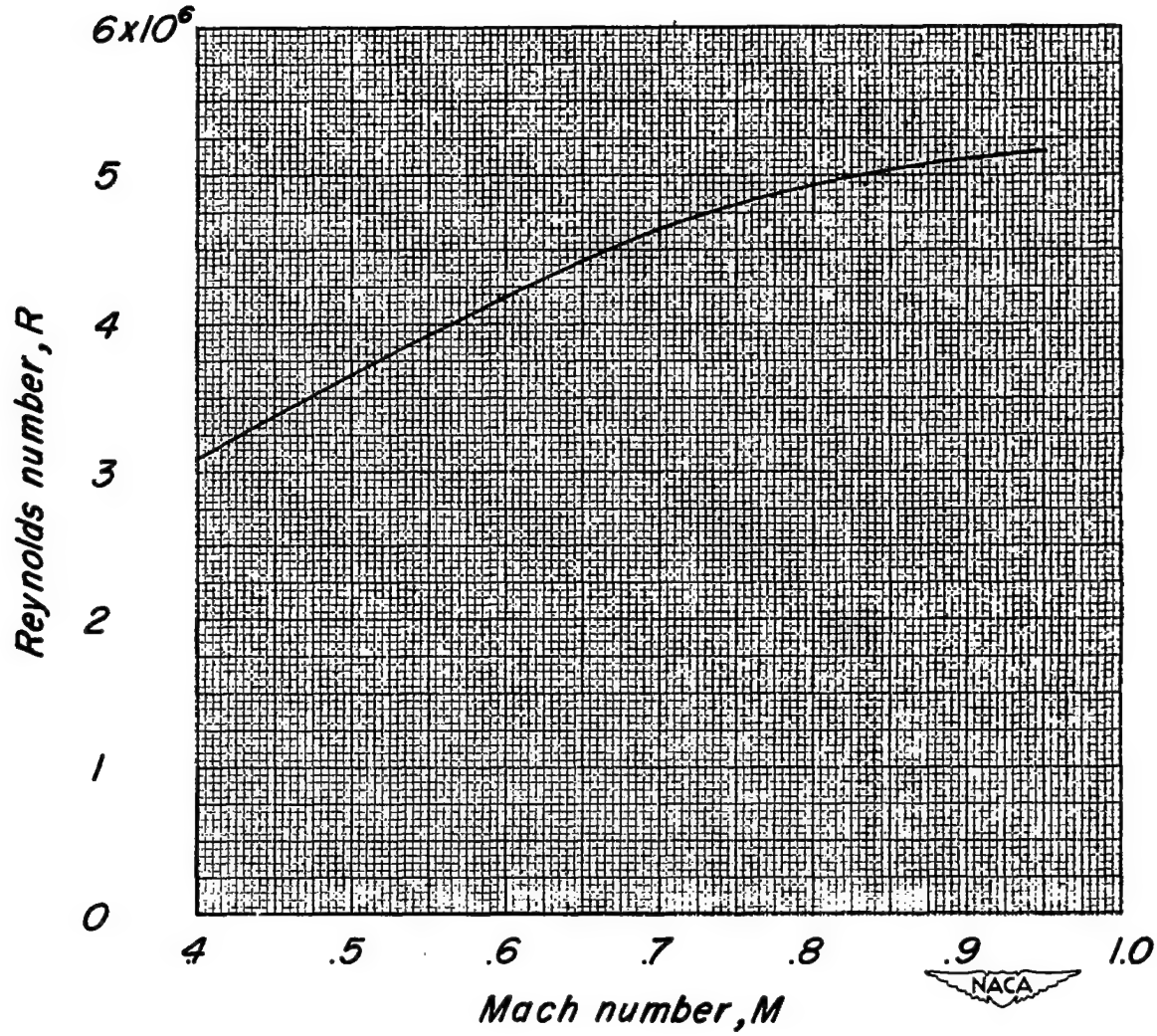

Figure 6.- Variation of mean test Reynolds number with Mach number based on the wing mean aerodynamic chord of 1.316 feet.

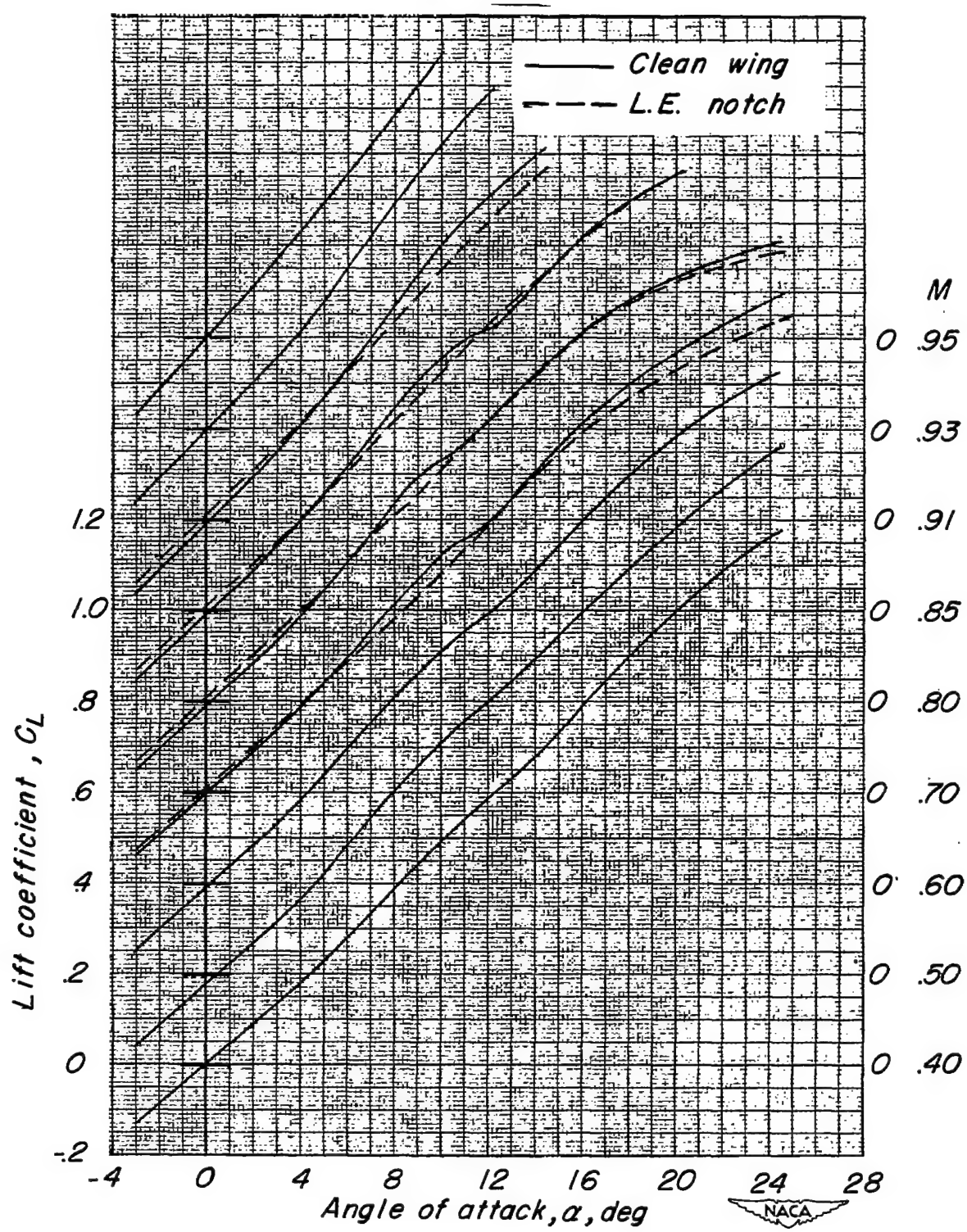

Figure 7.- Variation of lift coefficient C_L with angle of attack α throughout the test Mach number range.

[redacted]

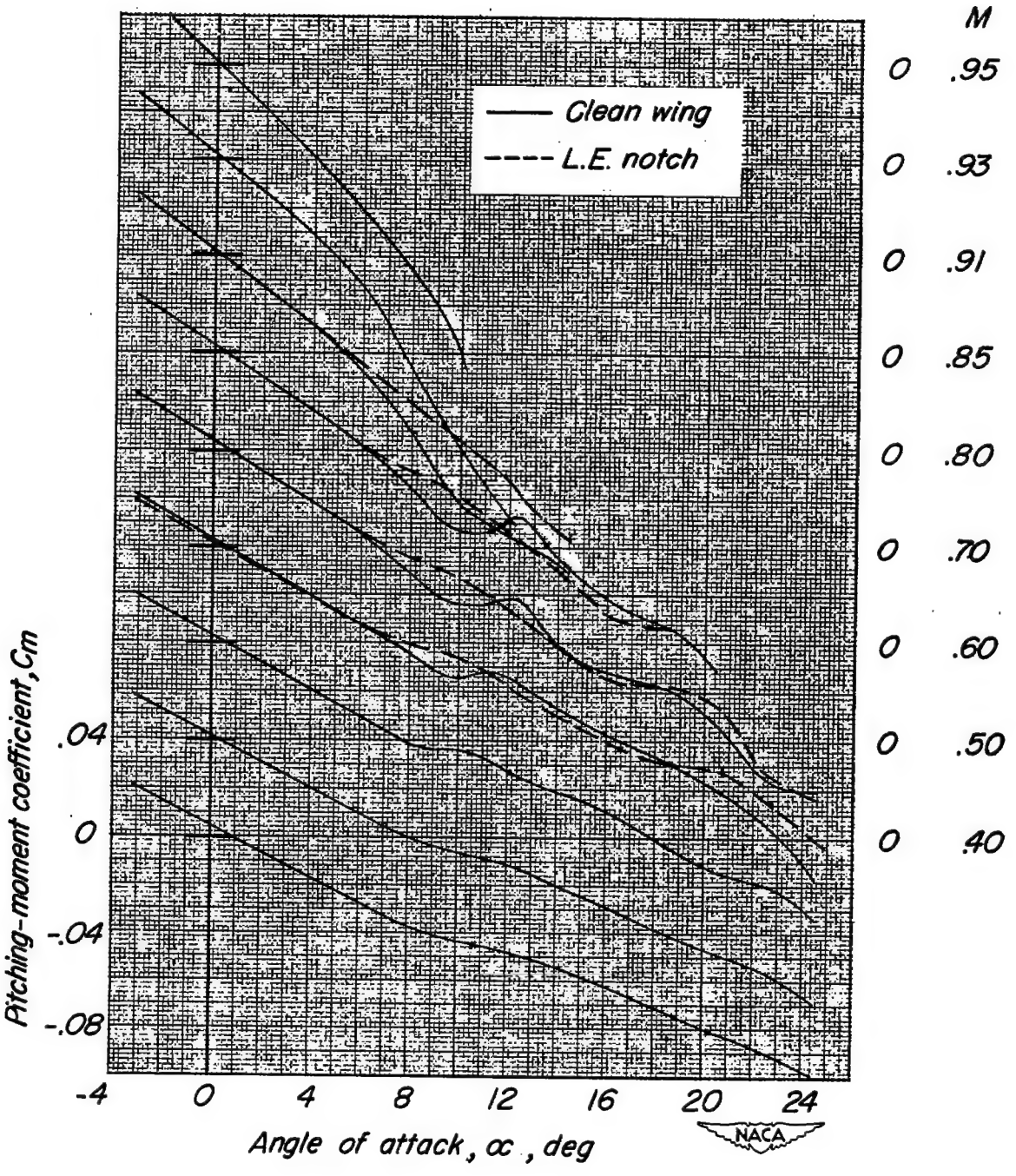

Figure 8.- Variation of pitching-moment coefficient C_m with angle of attack α throughout the test Mach number range.

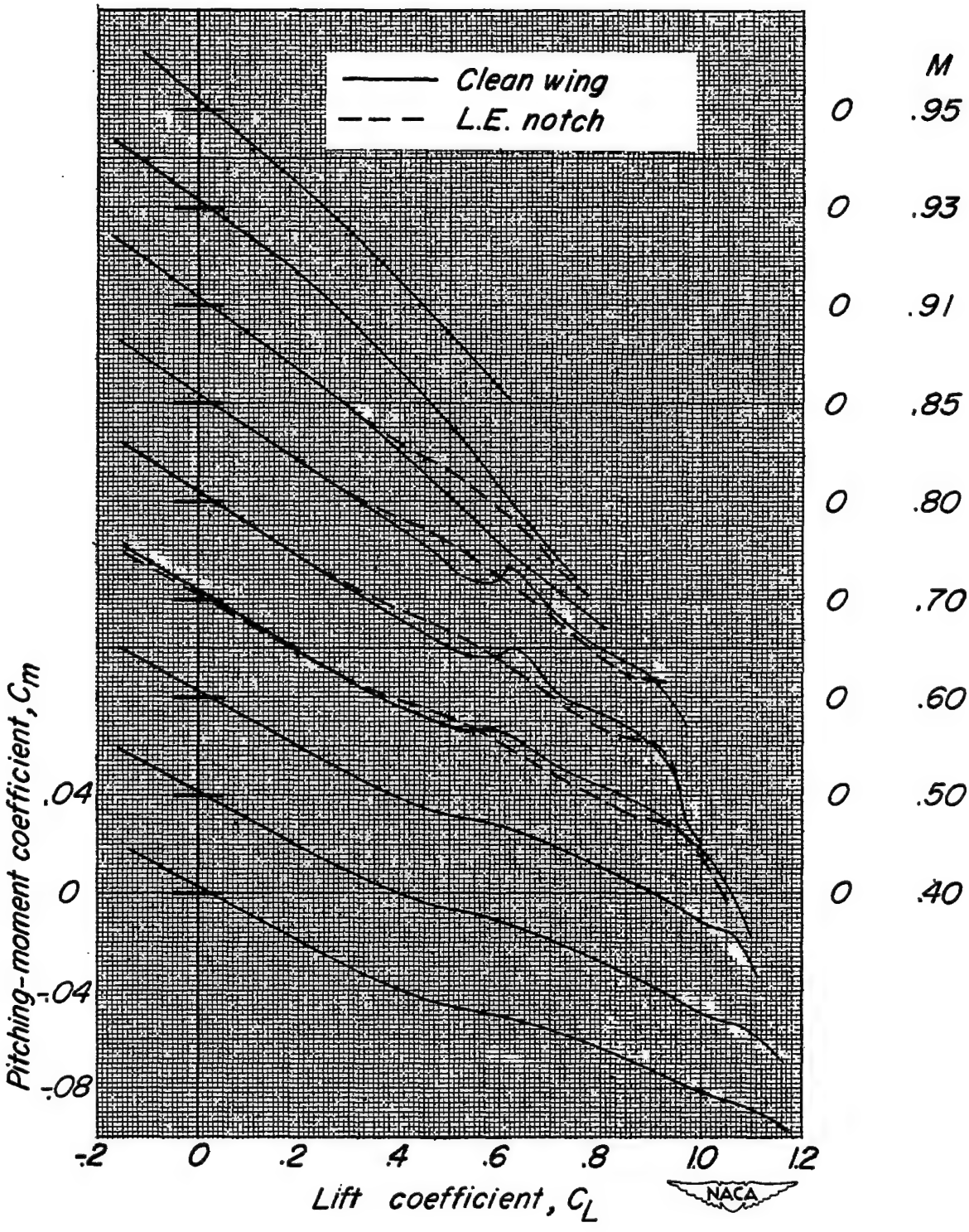

Figure 9.- Variation of pitching moment C_m with lift coefficient C_L throughout the test Mach number range.

[redacted]

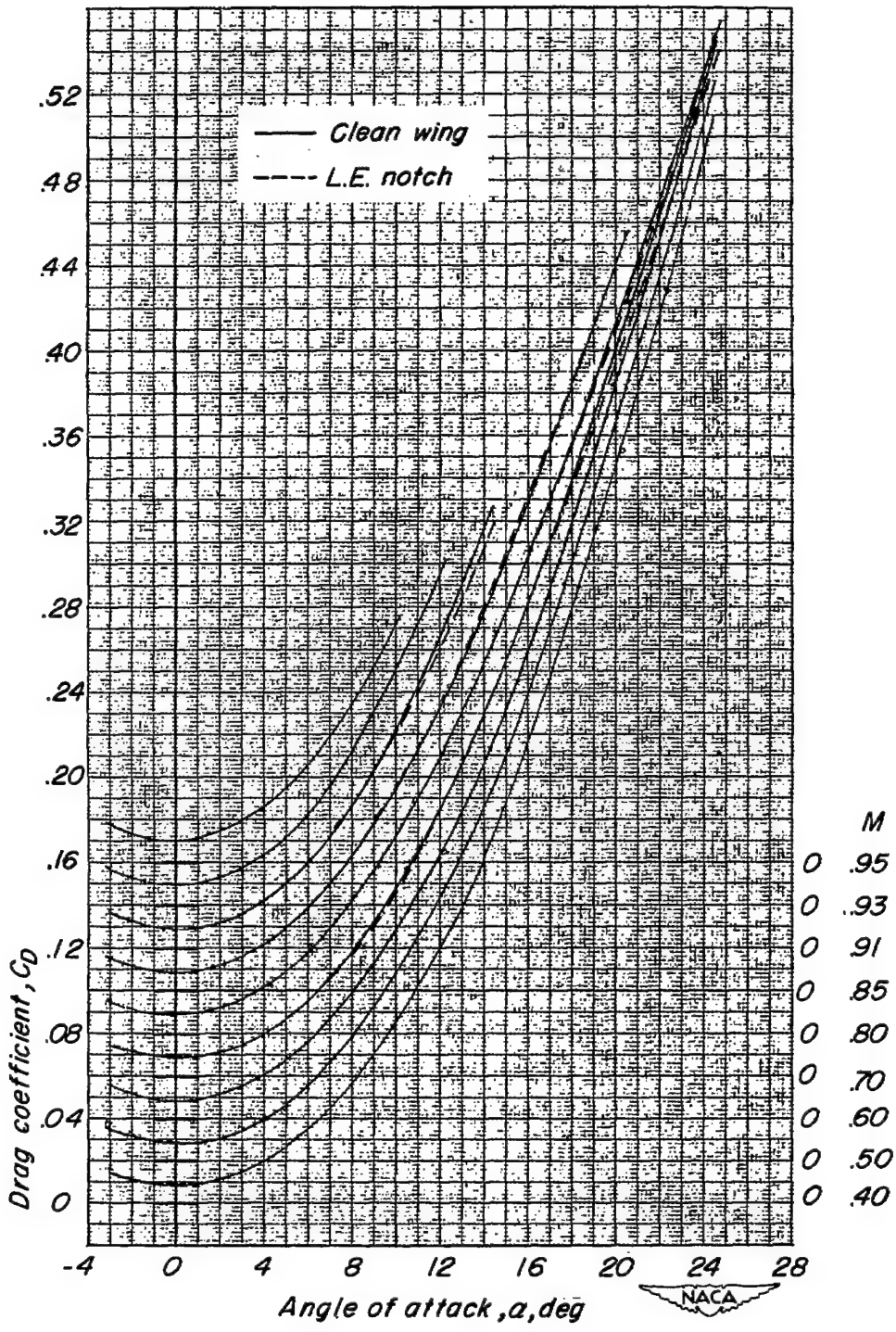

Figure 10.- Variation of drag coefficient with angle of attack throughout the test Mach number range. Data are corrected to free-stream static pressure at fuselage base but are not corrected for sting-interference tare.

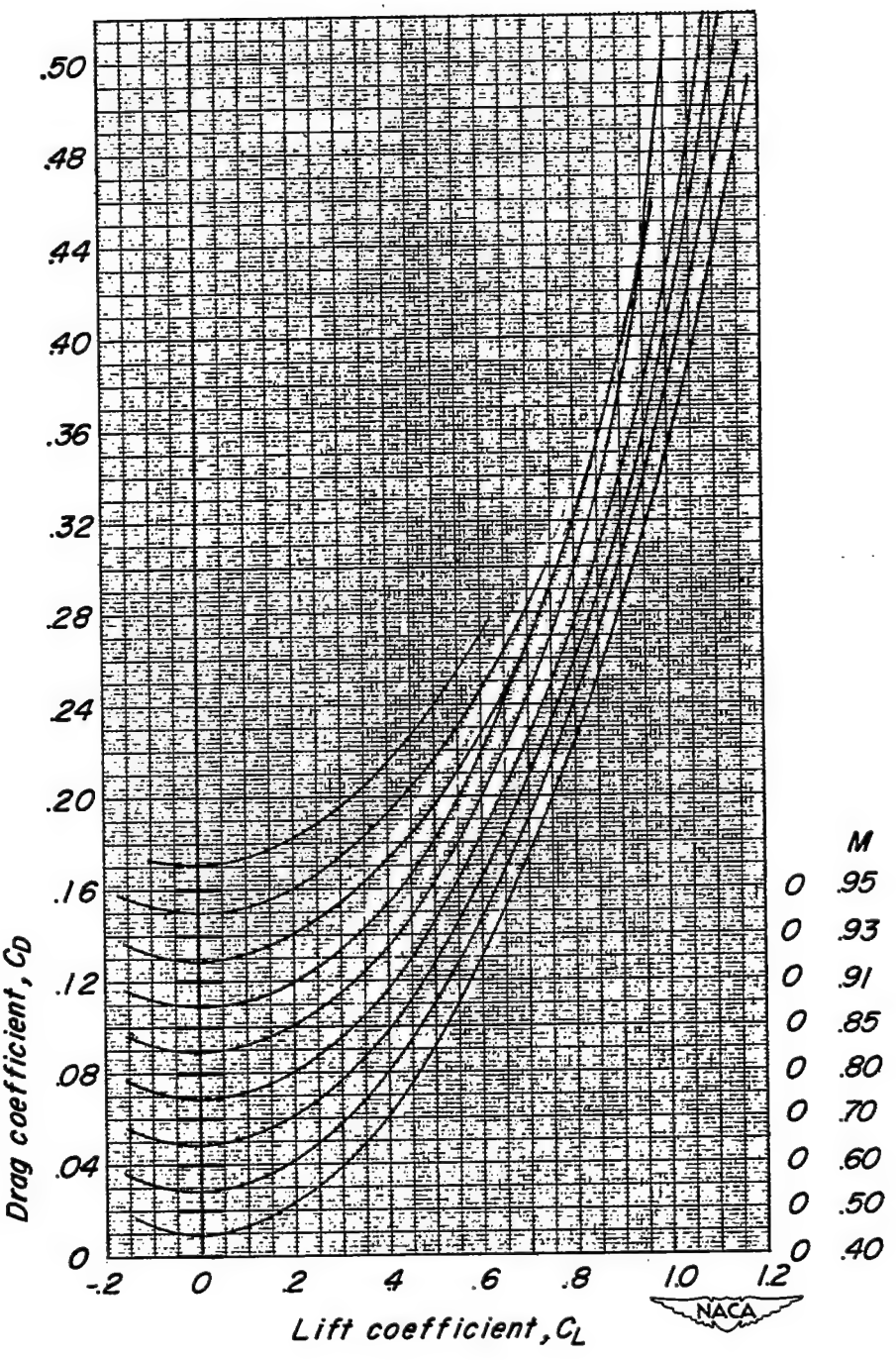

(a) Clean wing.

Figure 11.- Variation of drag coefficient with lift coefficient throughout the test Mach number range. Data are corrected to free-stream static pressure at fuselage base but are not corrected for sting-interference tare.

[redacted]

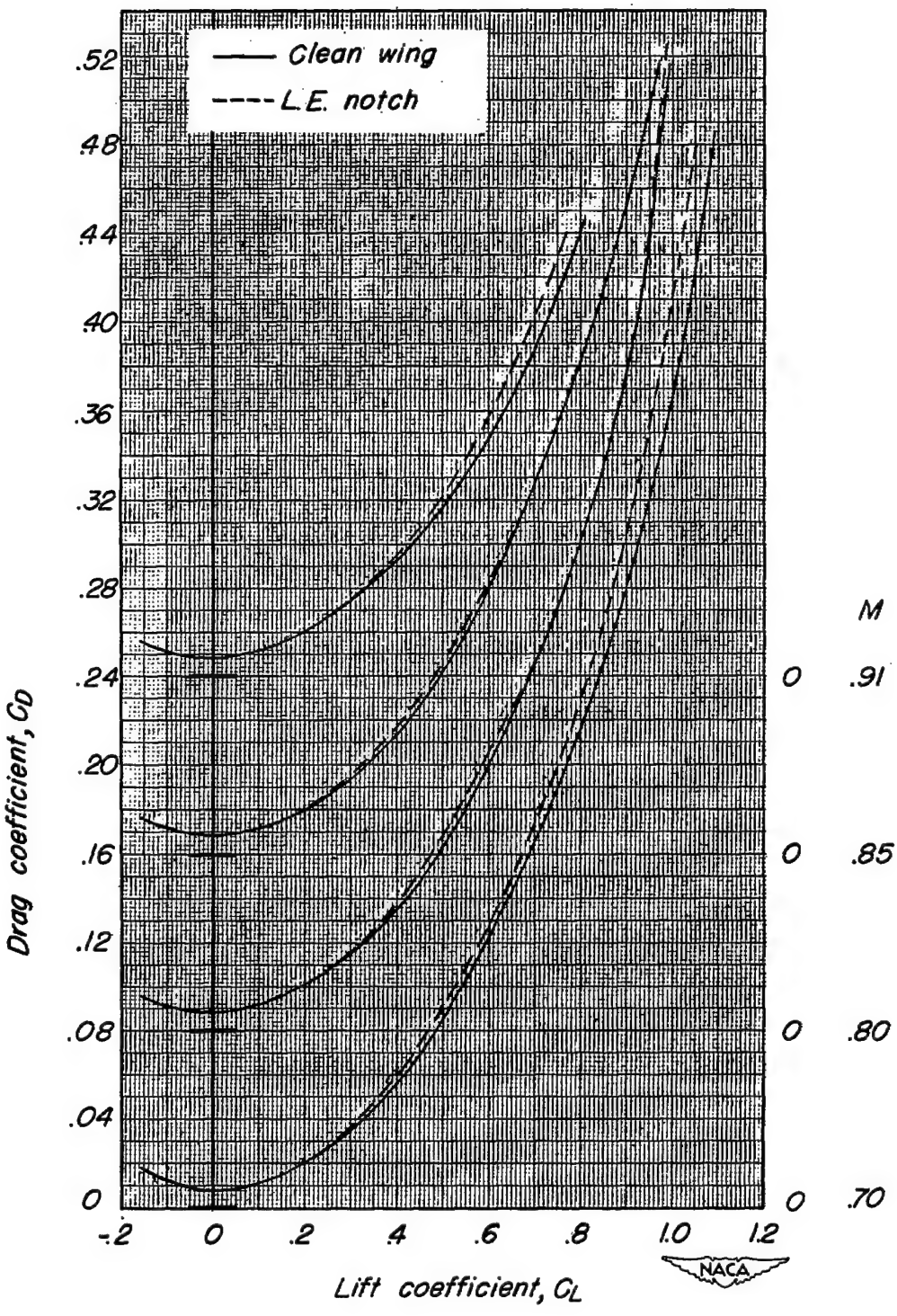

(b) Effect of leading-edge notch.

Figure 11.- Concluded.

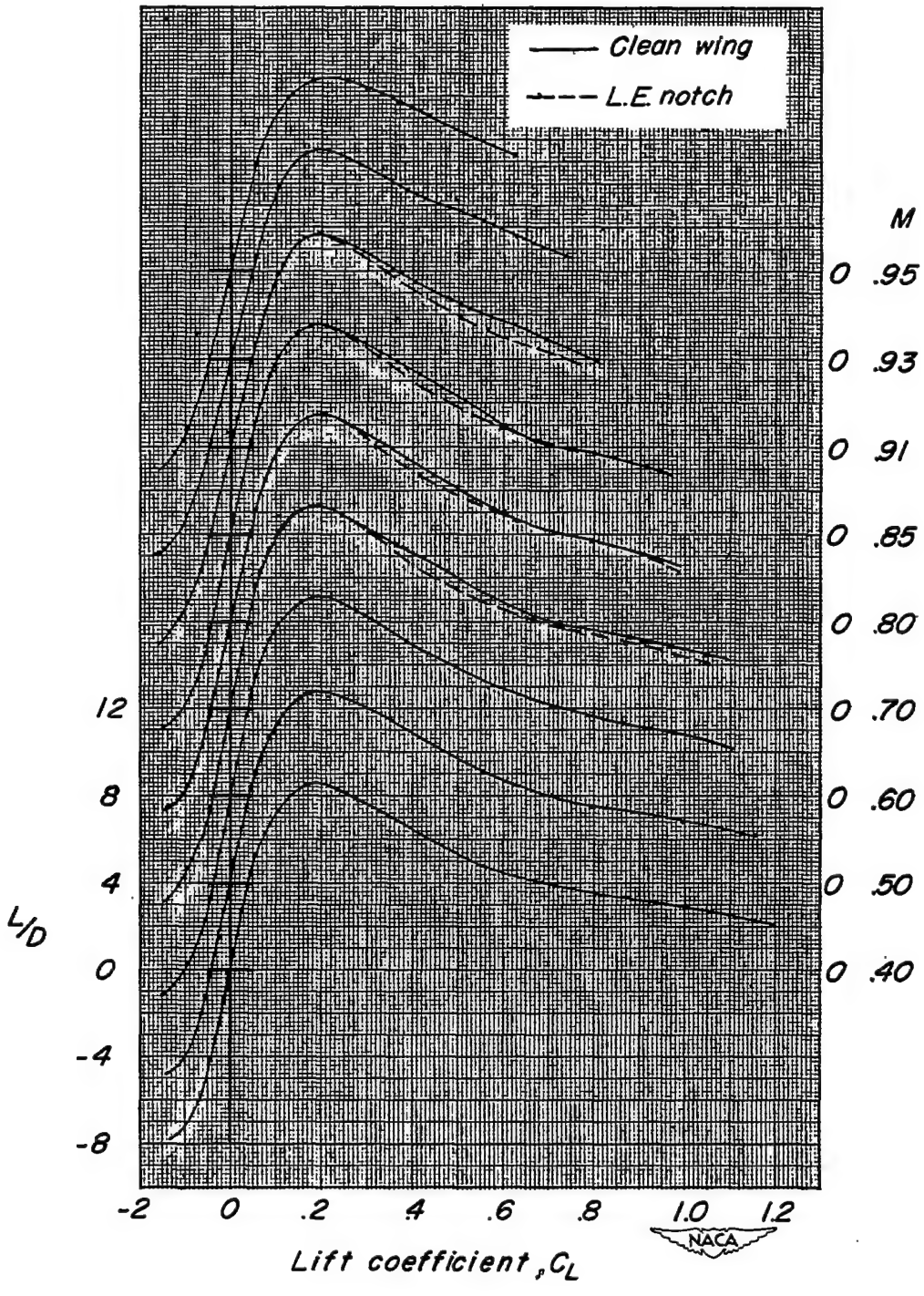

Figure 12.- Variation of lift-drag ratios L/D with lift coefficient C_L throughout the test Mach number range. Data are corrected to free-stream static pressure at fuselage base but are not corrected for sting-interference tare.

[redacted]

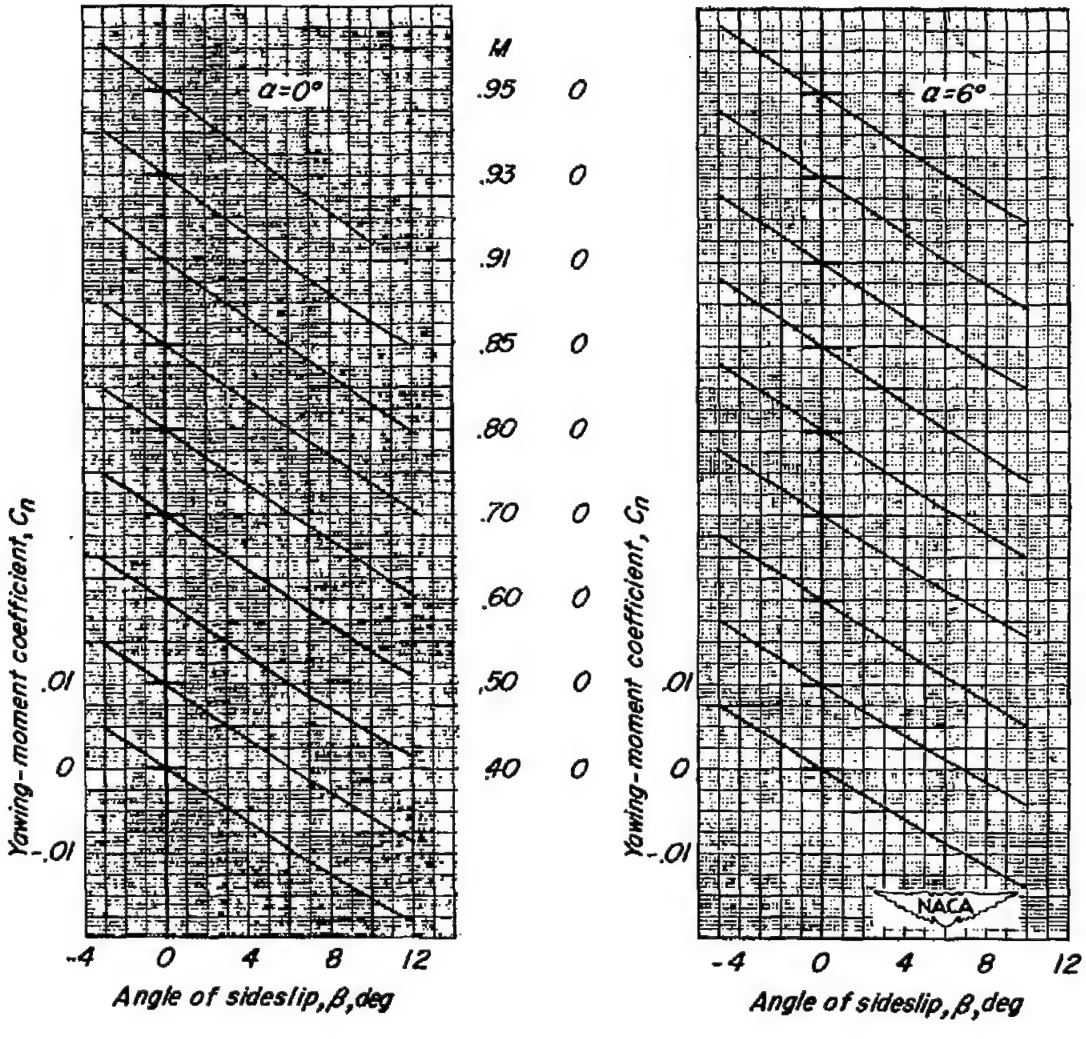

Figure 13.- Variation of yawing-moment coefficient C_n with angle of sideslip β throughout the test Mach number range at angles of attack of 0° and 6°.

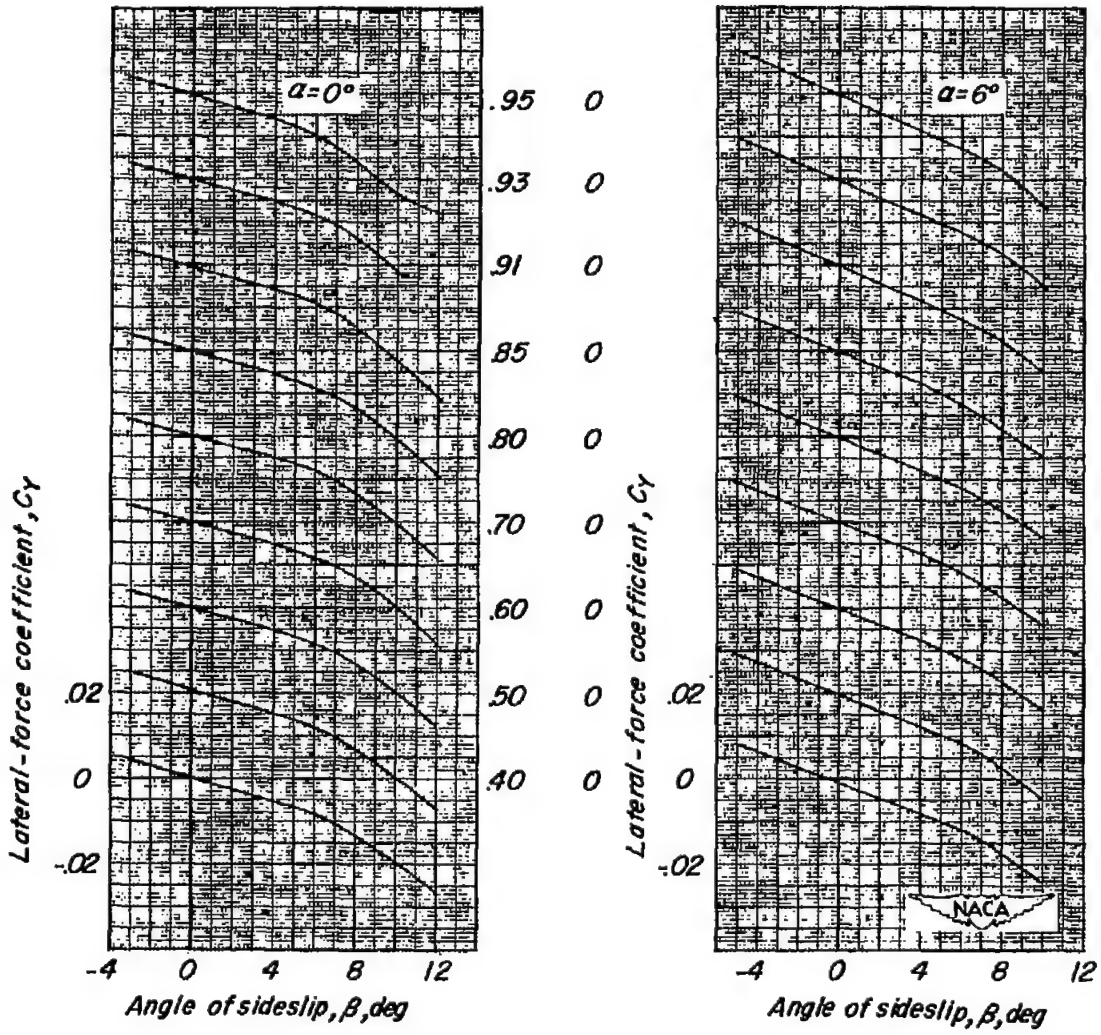

Figure 14.- Variation of lateral-force coefficient C_Y with angle of sideslip β throughout the test Mach number range at angles of attack of 0° and 6°.

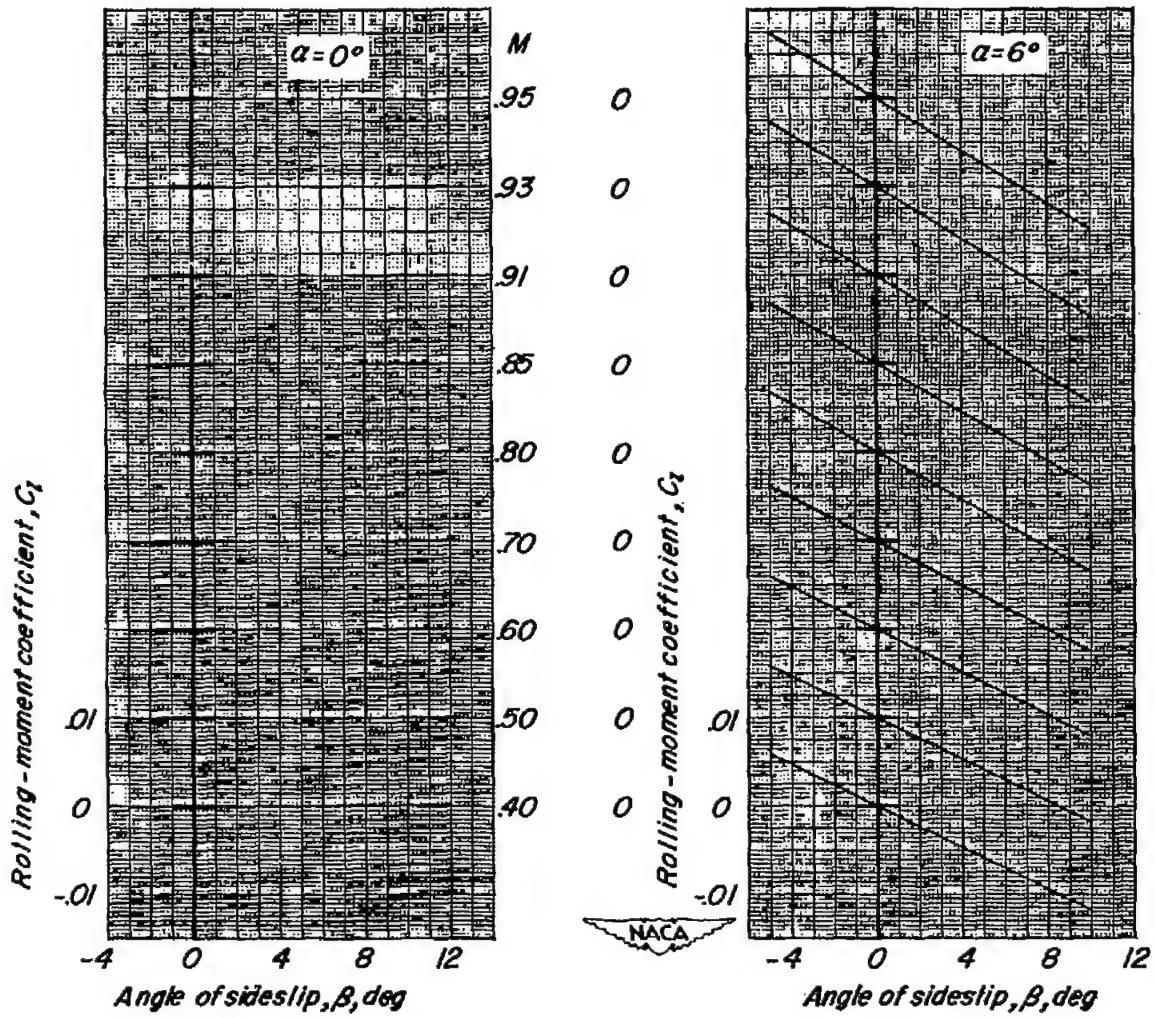

Figure 15.- Variation of rolling-moment coefficient C_l with angle of sideslip β throughout the test Mach number range at angles of attack of 0° and 6°.

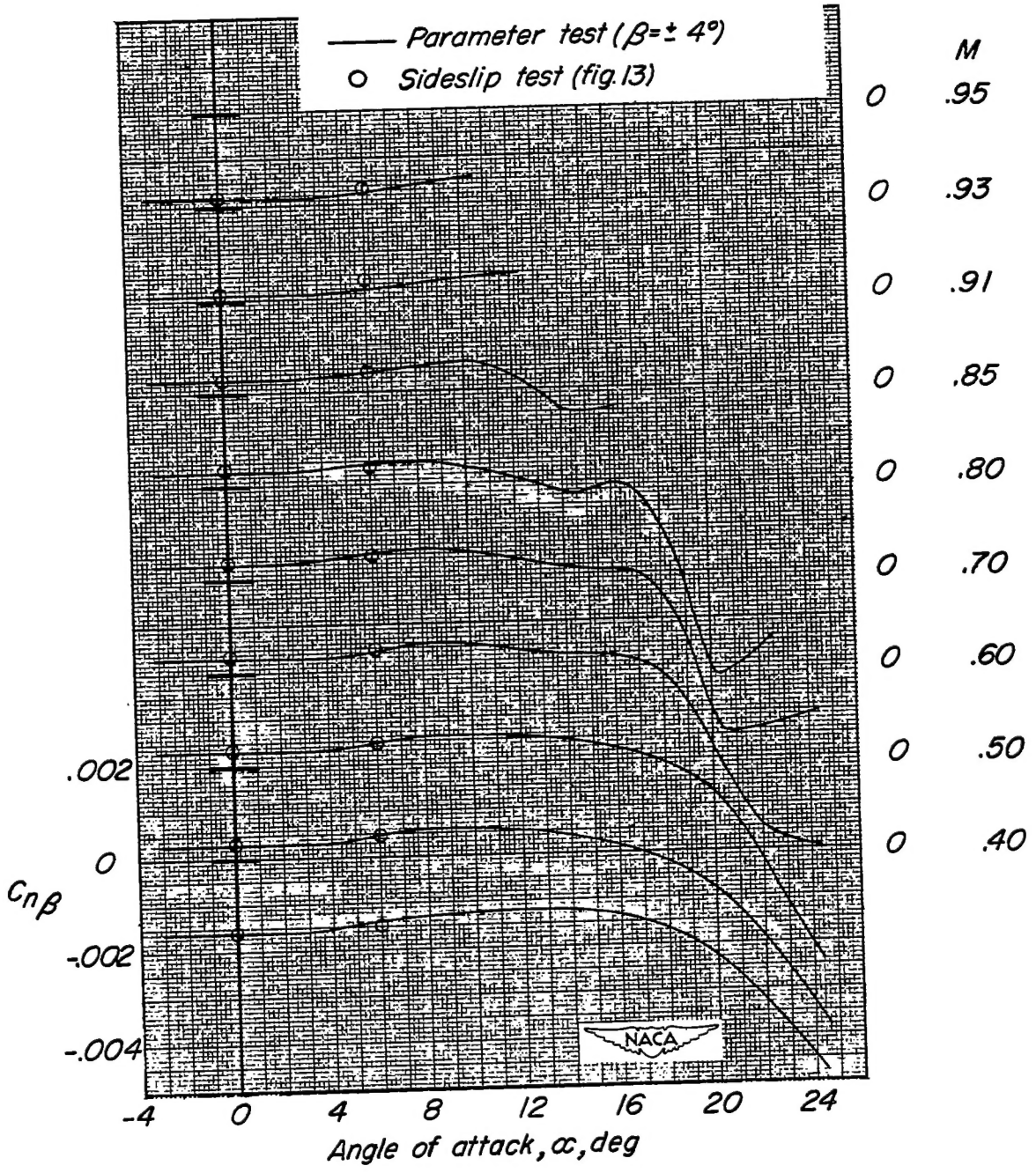

Figure 16.- Variation of the directional stability derivative $C_{n\beta}$ with angle of attack α throughout the test Mach number range.

[redacted]

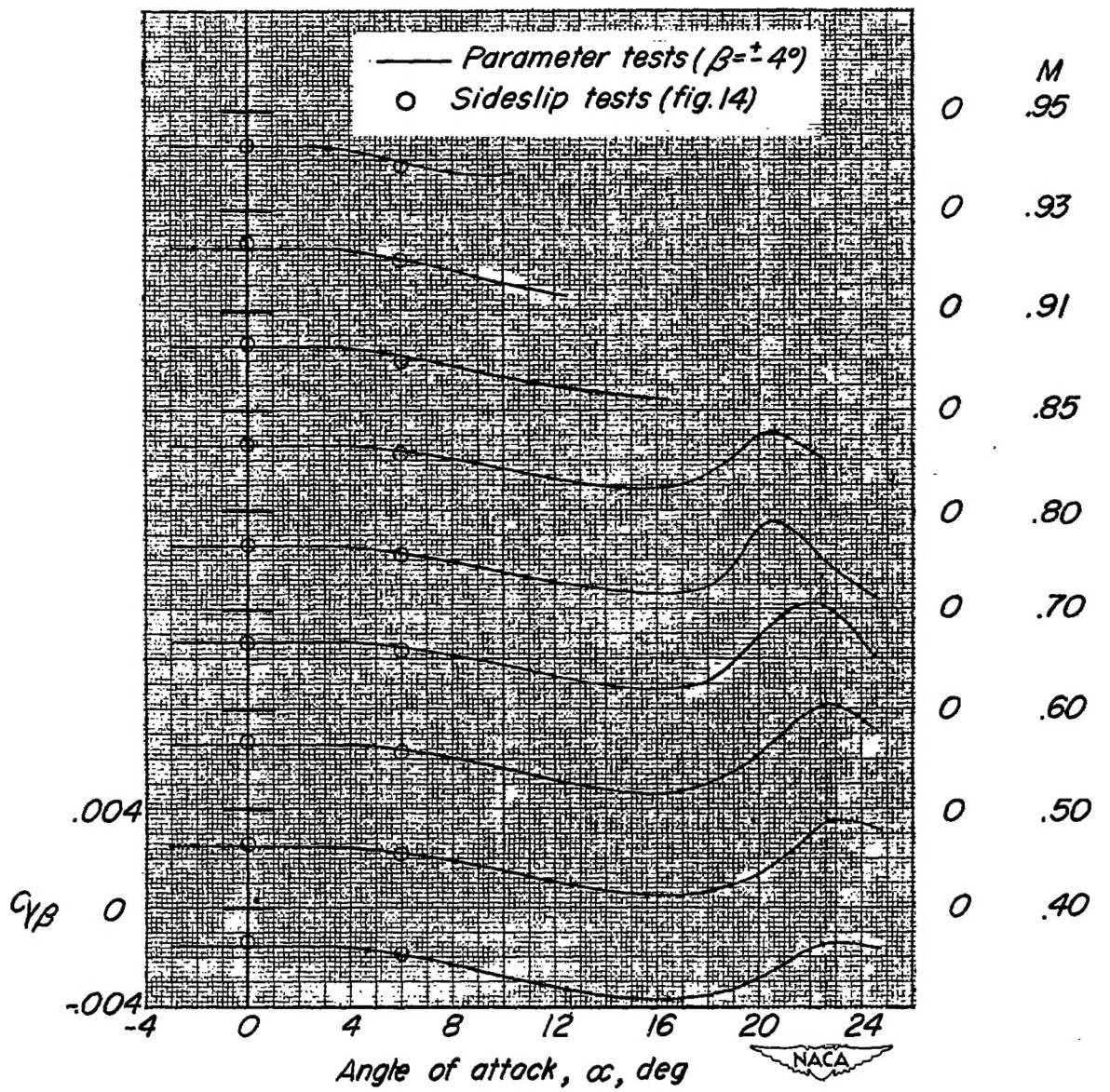

Figure 17.- Variation of the lateral-force derivative C_{Y_β} with angle of attack α throughout the test Mach number range.

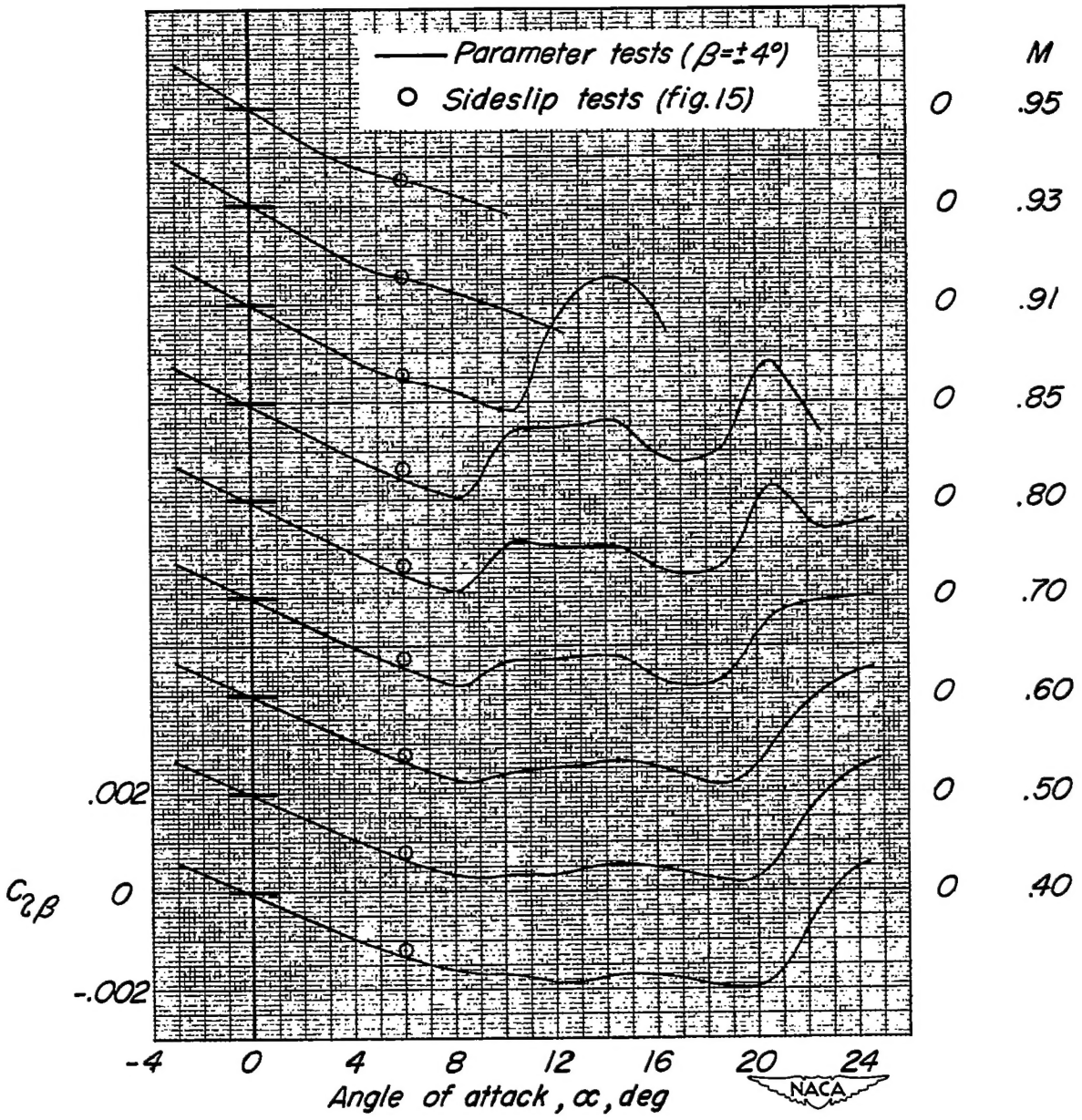

Figure 18.- Variation of effective dihedral C_{l_β} with angle of attack α throughout the test Mach number range.

[redacted]

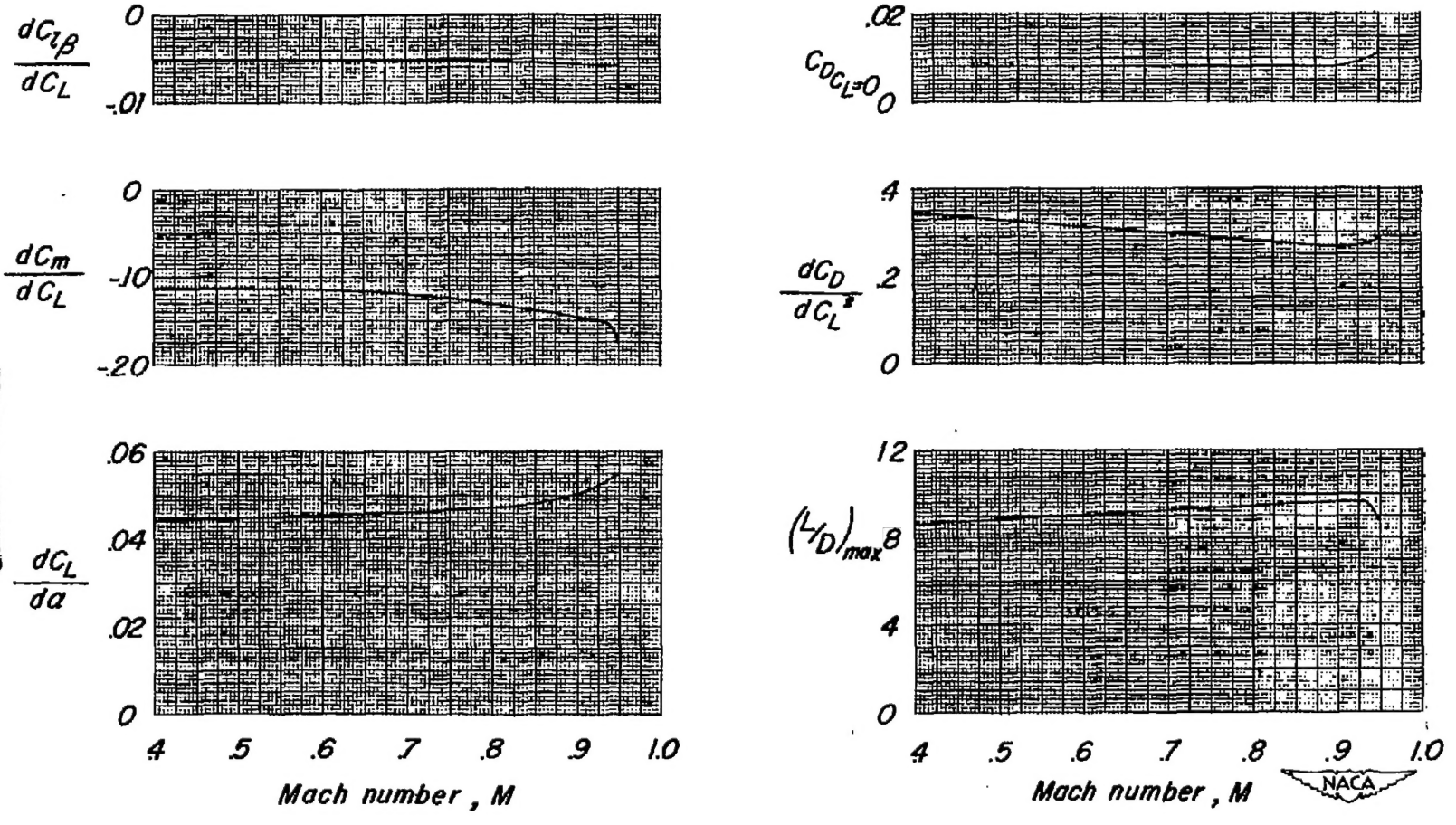

Figure 19.- Mach number effects on several parameters measured near an angle of attack of 0°. Drag data are corrected to free-stream static pressure at fuselage base but are not corrected for sting-interference tare.